

Supporting Information for

Ratiometric Fluorescence Imaging of Lysosomal Zn²⁺

Release under Oxidative Stress in Neural Stem Cells

Hao Zhu,^a Jiangli Fan,^{*a} Shiling Zhang,^a Jianfang Cao,^a Kedong Song,^b Dan Ge,^b
Huijuan Dong,^a Jingyun Wang,^b and Xiaojun Peng^{*a}

^a State Key Laboratory of Fine Chemicals, Dalian University of Technology, No. 2 Linggong Road,
High-tech District, Dalian 116024, China

^b School of Life Science and Biotechnology, Dalian University of Technology, Dalian, China.

Email: fanjl@dlut.edu.cn; pengxj@dlut.edu.cn

Content

Fig. S1 Effect of pH on fluorescence ratio of LysoZn-1 in ethanol/10 mM Tris-HCl = 4/6, v/v. ...	S3
Fig. S2 Fluorescence spectra of LysoZn-1 in the absence and presence of Zn ²⁺ and Cd ²⁺	S3
Fig. S3 The charge numbers of atoms on 1 and LysoZn-1	S4
Fig. S4 Frontier molecular orbital plots of 1 , 1 +Cd ²⁺ , 1 +Zn ²⁺ , LysoZn-1 , LysoZn-1 +Cd ²⁺ and LysoZn-1 +Zn ²⁺	S5
Fig. S5 Fluorescence spectra of 1 μM LysoZn-1 upon the titration of Zn ²⁺ (0-10 μM).....	S8
Fig. S6 Curve of fluorescence intensity of LysoZn-1 versus Zn ²⁺ concentration	S8
Fig. S7 Curve of fluorescence ratio of LysoZn-1 versus Zn ²⁺ concentration	S9
Fig. S8 Fluorescence intensity of LysoZn-1 versus log[Zn ²⁺] concentration.....	S9
Fig. S9 Fluorescence ratio of LysoZn-1 versus log[Zn ²⁺] concentration	S10
Fig. S10 Fluorescence spectra of LysoZn-1 upon the titration of Zn ²⁺ in acidic solution.....	S10
Fig. S11 Curve of fluorescence intensity of LysoZn-1 versus Zn ²⁺ concentration at pH 5.0.....	S11
Fig. S12 Curve of fluorescence ratio of LysoZn-1 versus Zn ²⁺ concentration at pH 5.0.....	S11
Fig. S13 The time courses of fluorescence intensity of LysoZn-1 in the presence of Zn ²⁺	S12
Fig. S14 Fluorescence responses of LysoZn-1 toward various cations at pH 7.2	S12
Fig. S15 Fluorescence responses of LysoZn-1 toward various anions at pH 5.0	S13
Fig. S16 Fluorescence responses of LysoZn-1 toward various anions at pH 7.2	S13
Fig. S17 Fluorescence ratio images of LysoZn-1 labelled MCF-7 cells in the presence of chloroquine	S14
Fig. S18 Zn ²⁺ -dependent ratio changes of LysoZn-1 in NSCs.....	S14
Fig. S19 Zn ²⁺ -dependent ratio changes of LysoZn-1 in MCF-7 cells.	S15
Fig. S20 Ratiometric imaging of Zn ²⁺ in LysoZn-1 labeled MCF-7 cells.....	S16
Fig. S21 Fluorescence spectra of LysoZn-1 and LysoZn-1 +H ₂ O ₂ at pH 5.0.	S16
Fig. S22 Cytotoxicity of LysoZn-1 on NSCs and MCF-7 cells.	S17
Fig. S23 ¹ H-NMR of 2	S17
Fig. S24 ¹³ C-NMR of 2	S18
Fig. S25 ¹ H-NMR of 3	S18
Fig. S26 ¹³ C-NMR of 3	S19

Fig. S27 ^1H -NMR of LysoZn-1	S19
Fig. S28 ^{13}C -NMR of LysoZn-1	S20

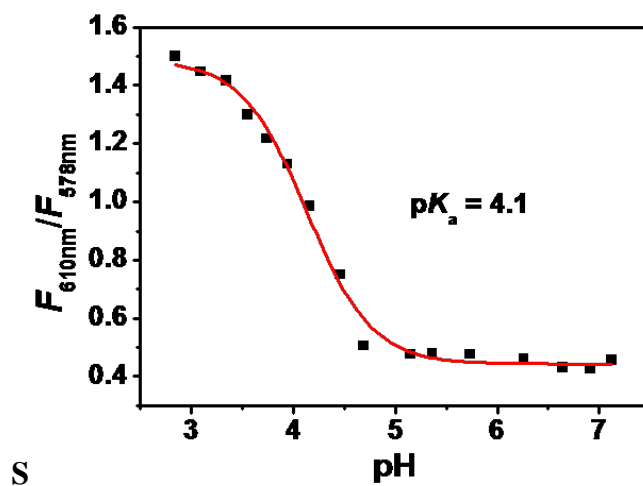


Fig. S1 Fluorescence ratio ($F_{610\text{nm}}/F_{578\text{nm}}$) of LysoZn-1 (1 μM) changes as a function of pH in ethanol/10 mM Tris-HCl = 4/6, v/v. Excitation wavelength was 545 nm.

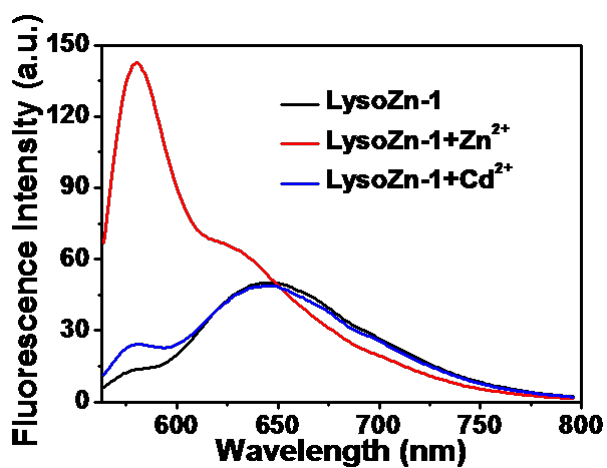


Fig. S2 Fluorescence spectra of 1 μM LysoZn-1 in the absence (black line) and presence of 200 μM Zn^{2+} (red line) and Cd^{2+} (blue line) in ethanol/50 mM $\text{CH}_3\text{COOH}-\text{CH}_3\text{COONa}$ = 9/1, v/v, pH 5.0.

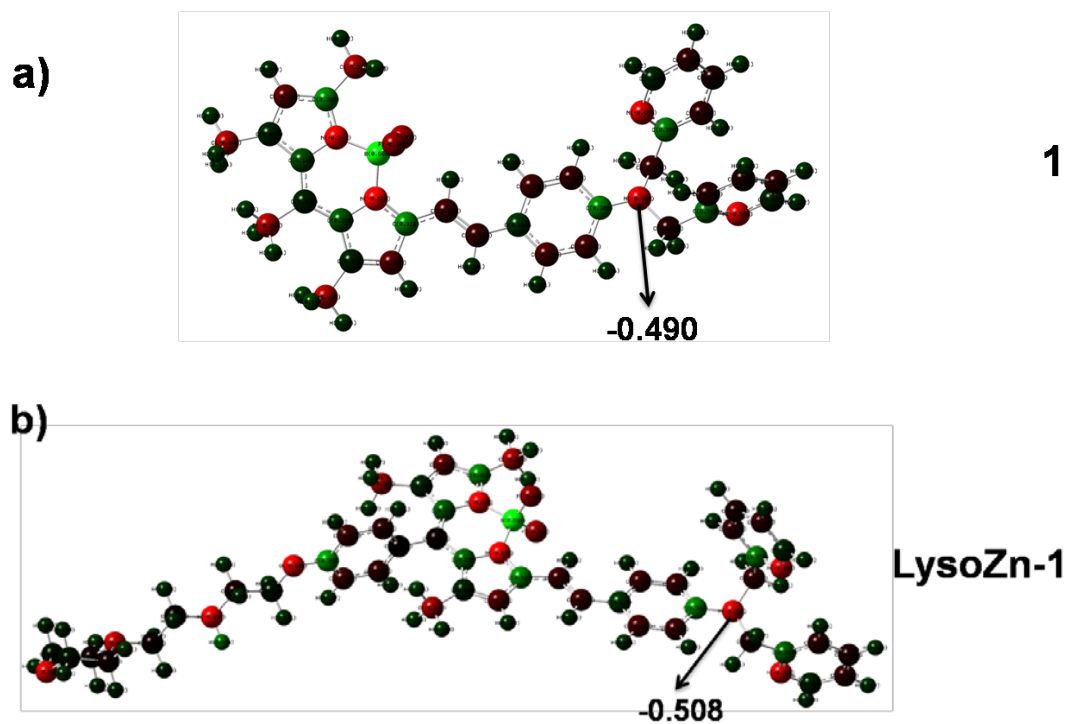
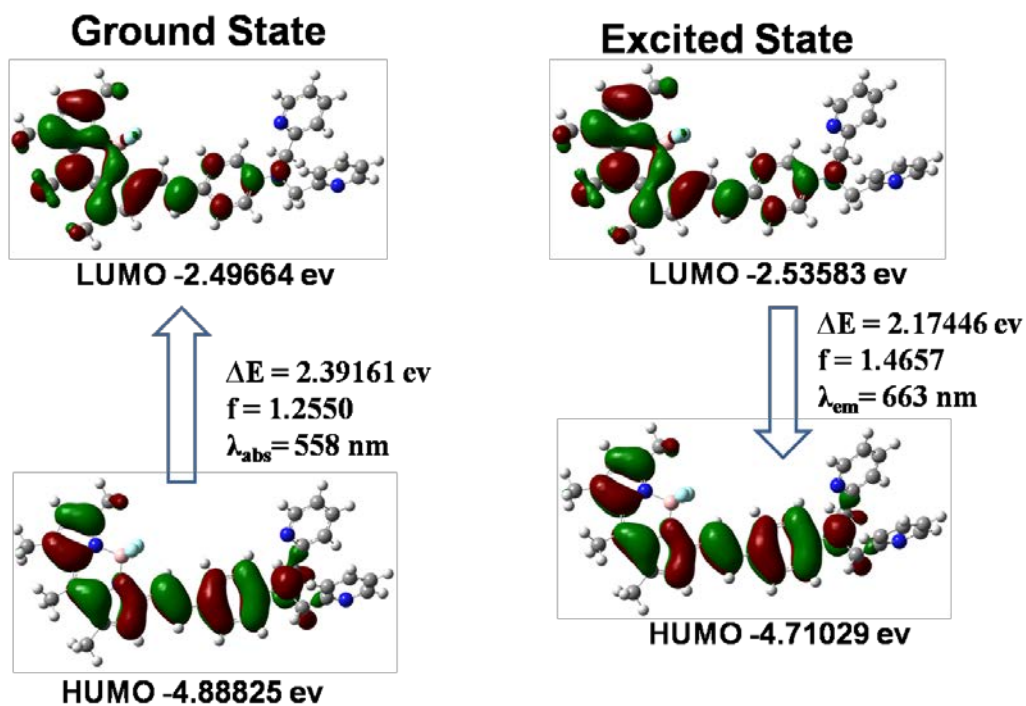


Fig. S3 The charge numbers of atoms on **1** (a) and **LysoZn-1** (b), respectively, calculated by method of DFT (B3LYP/6-31g(d, p)) using Gaussian 09. The arrow pointed number indicate the charge numbers of the tertiary amine nitrogen atom of DPA in **1** and **LysoZn-1**.

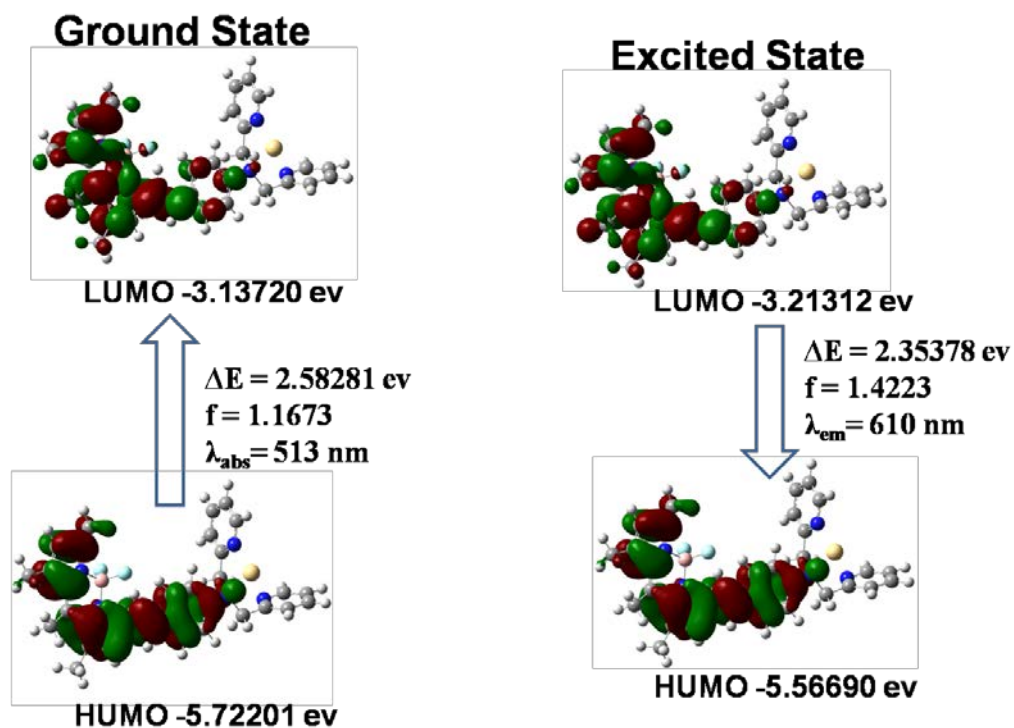
1

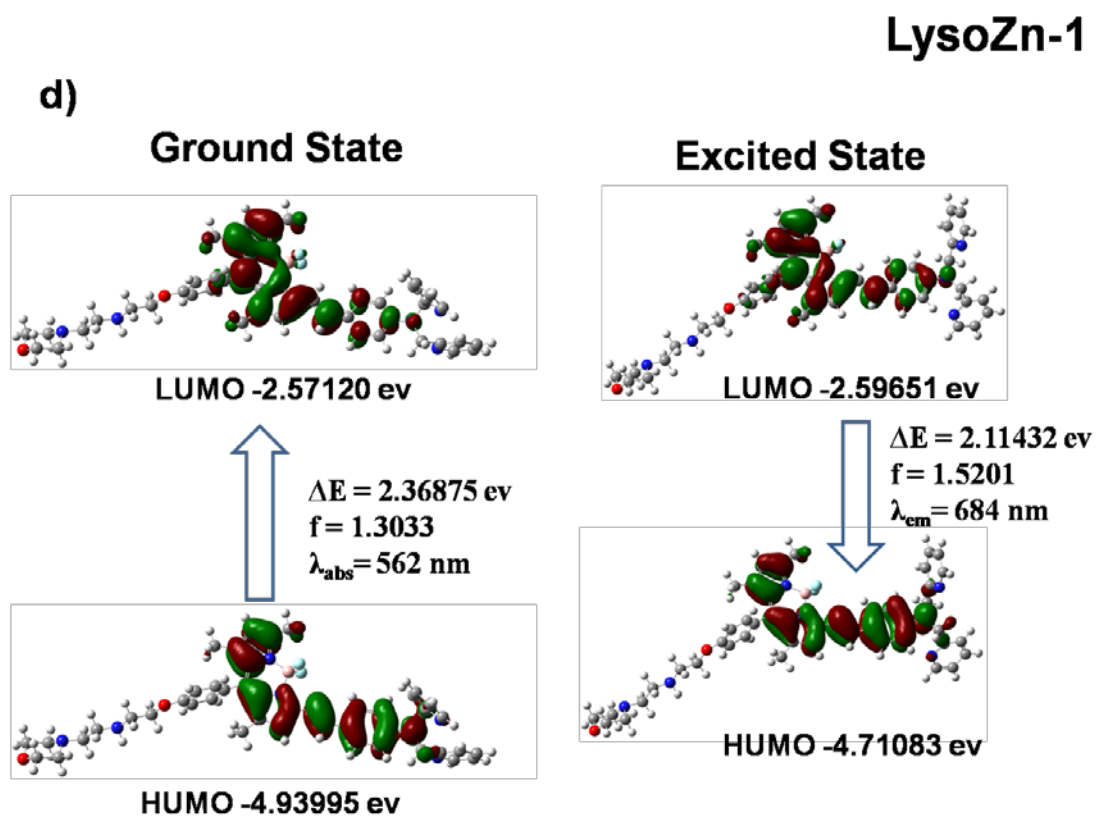
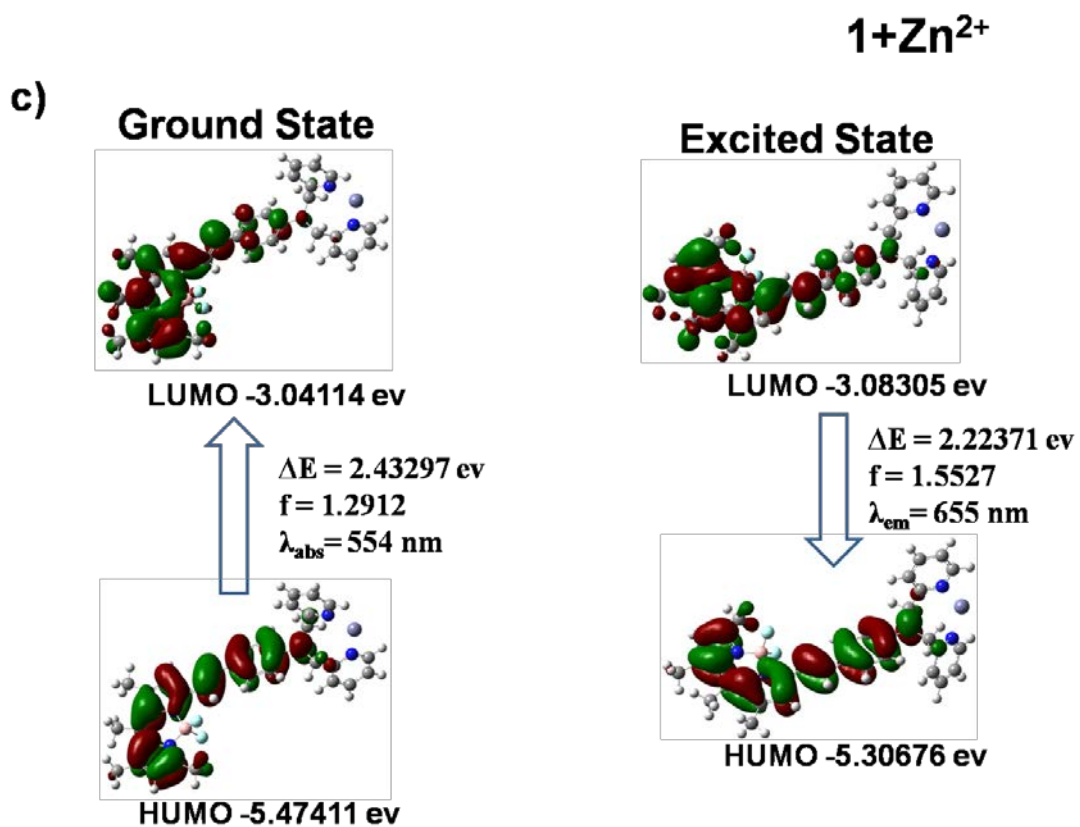
a)



1+Cd²⁺

b)





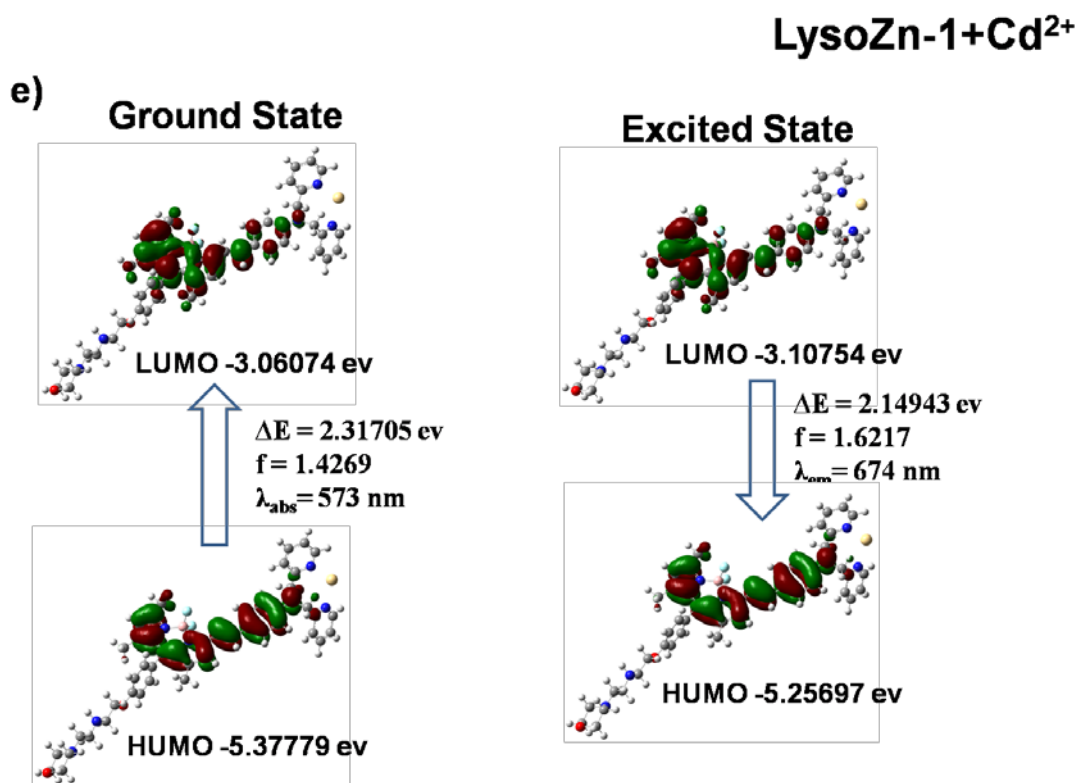


Fig. S4 Frontier molecular orbital plots of **1** (a), **1+Cd²⁺** (b), **1+Zn²⁺** (c), **LysoZn-1** (d), **LysoZn-1+Cd²⁺** (e), **LysoZn-1+Zn²⁺** (f); it is involved in the vertical excitation (UV/Vis

absorption, left column) and emission (right column). The vertical excitation related calculations are based on the optimised geometry of the ground state, and the emission related calculations were based on the optimised geometry of the excited state. B3LYP geometries and 6-31G (d, p) / LanL2DZ (for complex of **1**/LysoZn-1 with Cd²⁺ or Zn²⁺) basis set during the TD-DFT calculations.

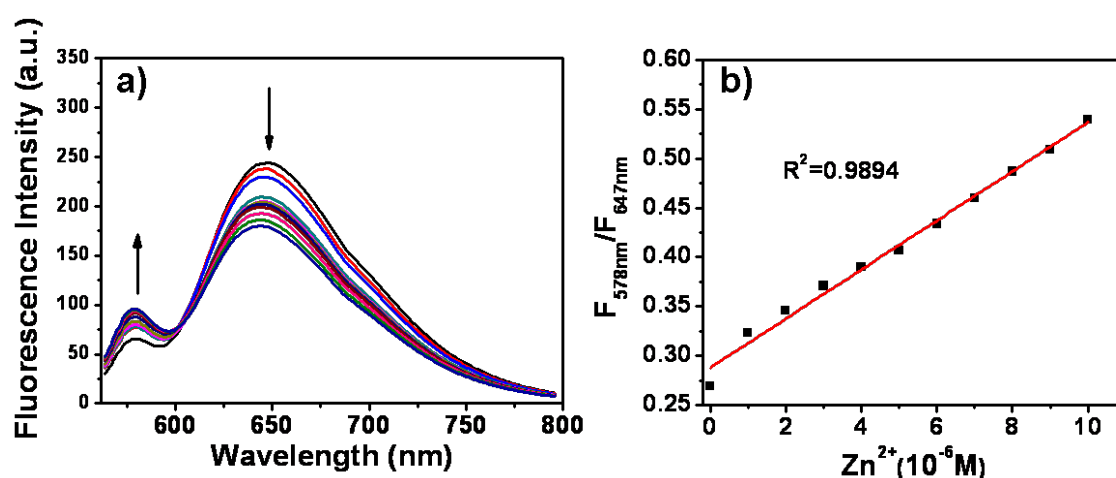


Fig. S5 a) Fluorescence spectra of 1 μM LysoZn-1 upon the titration of Zn²⁺ (0-10 μM) in ethanol/10 mM Tris-HCl = 9/1, v/v, pH 7.2. b) Fluorescence ratio ($F_{578\text{nm}}/F_{647\text{nm}}$) changes as a function of Zn²⁺ concentration (0-10 μM). Excitation wavelength was 545 nm.

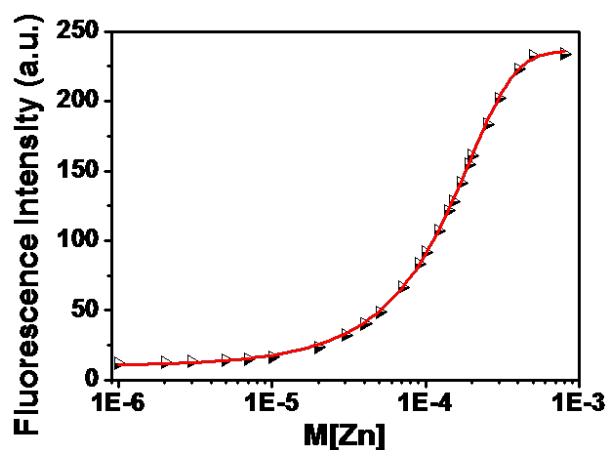


Fig. S6 Curve of fluorescence intensity at 578 nm ($F_{578\text{nm}}$) of LysoZn-1 versus increasing

concentration of Zn^{2+} . The concentration of **LysoZn-1** was $1 \mu\text{M}$. The dissociation constant K_d is deduced to be $6.8 \pm 0.4 \times 10^{-5} \text{ M}$.

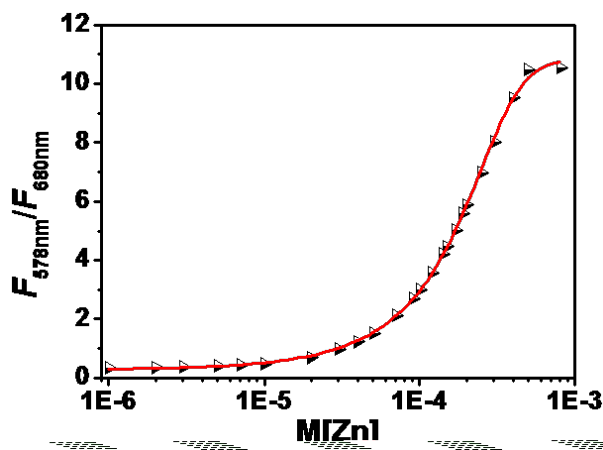


Fig. S7 Curve of fluorescence ratio ($F_{578\text{nm}}/F_{680\text{nm}}$) of **LysoZn-1** versus increasing concentration of Zn^{2+} . The concentration of **LysoZn-1** was $1 \mu\text{M}$. The dissociation constant K_d is deduced to be $12.3 \pm 0.6 \times 10^{-5} \text{ M}$.

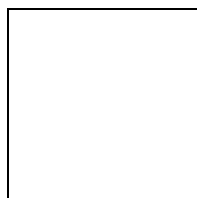


Fig. S8 Fluorescence intensity at 578 nm ($F_{578\text{nm}}$) of **LysoZn-1** versus increasing concentration of $\log[\text{Zn}^{2+}]$. The concentration of **LysoZn-1** was $1 \mu\text{M}$. The fluorescence response fits to a Hill coefficient of 1(1.09046). It is consistent with the formation of a 1:1 stoichiometry for the **LysoZn-1-Zn²⁺** complex.

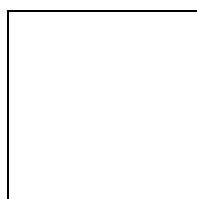


Fig. S9 Fluorescence ratio ($F_{578\text{nm}}/F_{680\text{nm}}$) of **LysoZn-1** versus increasing concentration of Zn^{2+} .

$\log[\text{Zn}^{2+}]$. The concentration of **LysoZn-1** was $1\ \mu\text{M}$. The fluorescence response fits to a Hill coefficient of 1(1.08136). It is consistent with the formation of a 1:1 stoichiometry for the **LysoZn-1-Zn²⁺** complex.

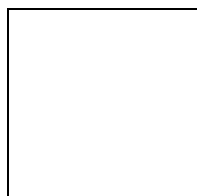


Fig. S10 Fluorescence spectra of $1\ \mu\text{M}$ **LysoZn-1** upon the titration of Zn^{2+} (0, 5, 10, 20, 30, 50, 70, 90, 120, 150, 180, 200, 230, 300, 400, 500, 600 and $800\ \mu\text{M}$) in ethanol/50 mM $\text{CH}_3\text{COOH-CH}_3\text{COONa} = 9/1$, v/v, pH 5.0. Excitation wavelength was 545 nm.

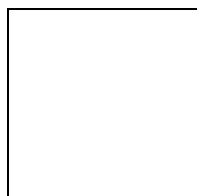


Fig. S11 Curve of fluorescence intensity at 578 nm ($F_{578\text{nm}}$) of **LysoZn-1** versus increasing concentration of Zn^{2+} at pH 5.0. The concentration of **LysoZn-1** was $1\ \mu\text{M}$. The dissociation constant K_d is deduced to be $8.1 \pm 0.9 \times 10^{-5}$ M.

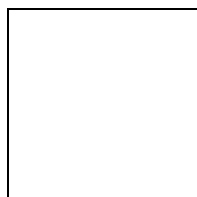


Fig. S12 Curve of fluorescence intensity ratio ($F_{578\text{nm}}/F_{680\text{nm}}$) of **LysoZn-1** versus increasing concentration of Zn^{2+} at pH 5.0. The concentration of **LysoZn-1** was $1\ \mu\text{M}$. The dissociation

constant K_d is deduced to be $16.0 \pm 0.7 \times 10^{-5}$ M.

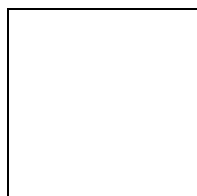


Fig. S13 The time courses of fluorescence intensity (578 nm) of **LysoZn-1** (1 μ M) in the presence of 200 μ M Zn^{2+} in ethanol/10 mM Tris-HCl = 9/1, v/v, pH 7.2. Excitation wavelength was 545 nm.

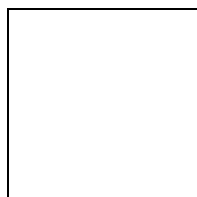


Fig. S14 Fluorescence responses of **LysoZn-1** (1 μ M) toward 200 μ M various cations in ethanol/10 mM Tris-HCl = 9/1, v/v, pH 7.2. From right to left: Ag^+ , Ba^{2+} , Ca^{2+} , Cd^{2+} , Cu^+ , Co^{2+} , Cr^{3+} , Fe^{3+} , Hg^{2+} , K^+ , Mg^{2+} , Mn^{2+} , Na^+ , Ni^{2+} , Pb^{2+} , Zn^{2+} . Excitation wavelength was 545 nm. Black bars represent the relative emission intensity (F/F_0 , at 578 nm) of **LysoZn-1**+cations; light gray bars represent the fluorescence intensity of **LysoZn-1**+ Zn^{2+} in the presence of other cations.

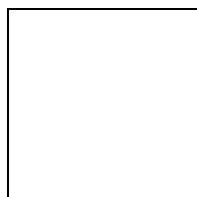


Fig. S15 Fluorescence responses of **LysoZn-1** (1 μ M) toward various anions (200 μ M) in ethanol/50 mM $CH_3COOH-CH_3COONa$ = 9/1, v/v, pH 5.0. From right to left: Br^- , CH_3COO^- , Cl^- ,

ClO^- , ClO_4^- , CO_3^{2-} , HPO_4^{2-} , H_2PO_4^- , Γ , NO_3^- , S^{2-} , Zn^{2+} . Excitation wavelength was 545 nm. Black bars represent the relative emission intensity (F/F_0 , at 578 nm) of **LysoZn-1**+anions; gray bars represent the fluorescence intensity of **LysoZn-1**+ Zn^{2+} in the presence of other anions.

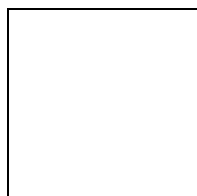


Fig. S16 Fluorescence responses of **LysoZn-1** (1 μM) toward various anions (200 μM) in ethanol/10 mM Tris-HCl = 9/1, v/v, pH 7.2. From right to left: Br^- , CH_3COO^- , Cl^- , ClO^- , ClO_4^- , CO_3^{2-} , HPO_4^{2-} , H_2PO_4^- , Γ , NO_3^- , S^{2-} , Zn^{2+} . Excitation wavelength was 545 nm. Black bars represent the relative emission intensity (F/F_0 , at 578 nm) of **LysoZn-1**+anions; gray bars represent the fluorescence intensity of **LysoZn-1**+ Zn^{2+} in the presence of other anions.

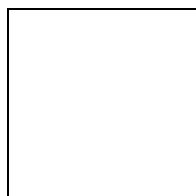


Fig. S17 Fluorescence ratio images ($F_{575-620 \text{ nm}}/F_{655-755 \text{ nm}}$) of **LysoZn-1** (1 μM) labelled MCF-7 cells in the presence of 100 μM chloroquine at different time points: a) 0 min; b) 5 min; c) 10 min; d) 15 min; e) 20 min; f) 25 min; g) 30 min. Excitation wavelength is 559 nm. h) Bright field. i) Plot of the emission ratios as a function of time after chloroquine was added. The ratio values are extracted from 7 regions of each image, error bars are $\pm\text{sem}$.

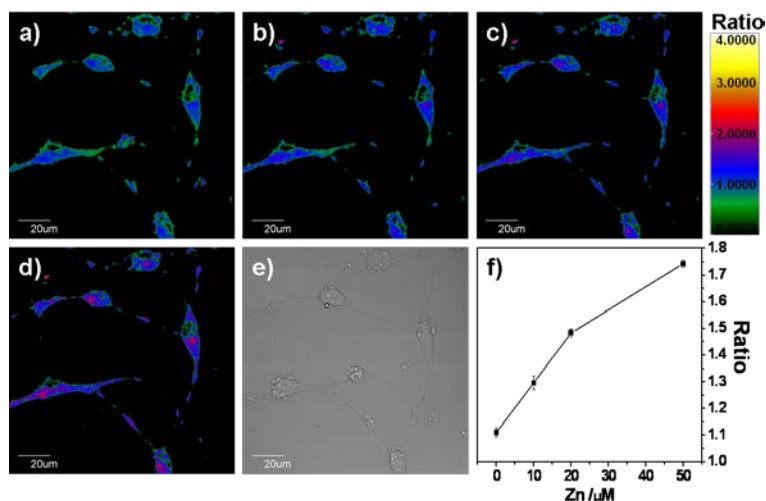


Fig. S18 Zn²⁺-dependent ratio changes of **LysoZn-1** in NSCs. Cells were treated with 1 μM **LysoZn-1** for 30 min, then various concentrations of Zn²⁺ was added: a) 0 μM; b) 10 μM; c) 20 μM; d) 50 μM. After 10 min incubation, confocal fluorescence images were recorded; e) bright field; f) fluorescence ratio ($F_{575-620\text{nm}}/F_{655-755\text{nm}}$) changes as a function of Zn²⁺ concentration upon 559 nm excitation. The ratio values are extracted from 5 regions of each image, error bars are \pm sem.

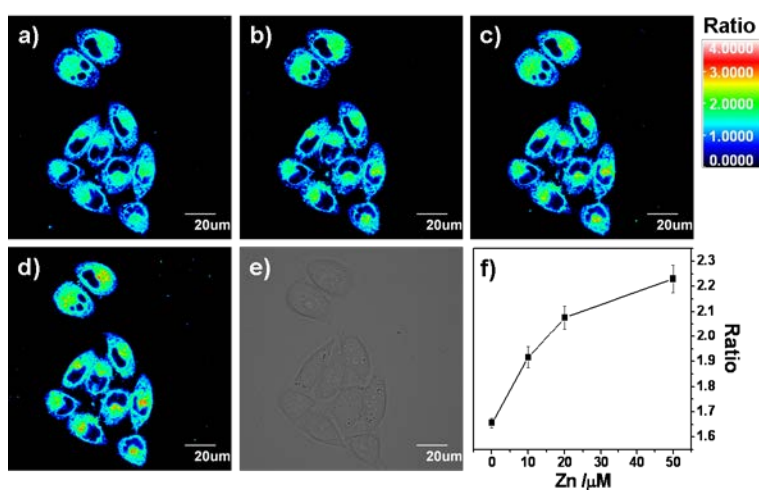


Fig. S19 Zn²⁺-dependent ratio changes of **LysoZn-1** in MCF-7 cells. Cells were treated with 1 μM **LysoZn-1** for 30 min, then various concentrations of Zn²⁺ was added: a) 0 μM; b) 10 μM;

c) 20 μM ; d) 50 μM . After 10 min incubation, confocal fluorescence images were recorded; e) bright field; f) fluorescence ratio ($F_{575-620 \text{ nm}}/F_{655-755 \text{ nm}}$) changes as a function of Zn^{2+} concentration upon 559 nm excitation. The ratio values are extracted from 10 regions of each image, error bars are $\pm\text{sem}$.

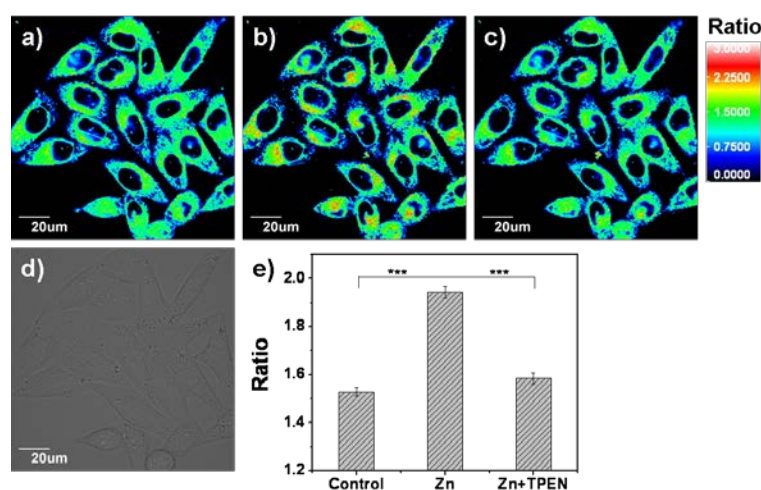


Fig. S20 Ratiometric imaging ($F_{575-620 \text{ nm}}/F_{655-755 \text{ nm}}$) of Zn^{2+} in **LysoZn-1** labeled MCF-7 cells.

a) Cells were incubated with 1 μM **LysoZn-1** for 30 min; b) following a 10 min treatment of Zn^{2+} (20 μM); c) fluorescence ratio images of cells in b) treated further by TPEN solution (20 μM , 10 min); d) bright field; e) statistical analyses were performed with One-Way ANOVA ($n = 13$ fields of cells). $***P < 0.001$, and error bars are $\pm\text{sem}$. Excitation wavelength is 559 nm.

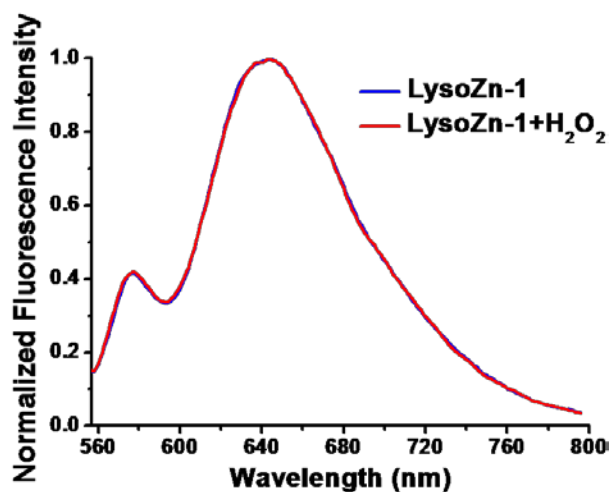


Fig. S21 Fluorescence spectra of **LysoZn-1** (blue line) and **LysoZn-1+H₂O₂** (red line) in ethanol/50 mM CH₃COOH-CH₃COONa = 9/1, v/v, pH 5.0. Excitation wavelength is 545 nm.

The concentrations of **LysoZn-1** and H₂O₂ were 1 μM and 1 mM, respectively.

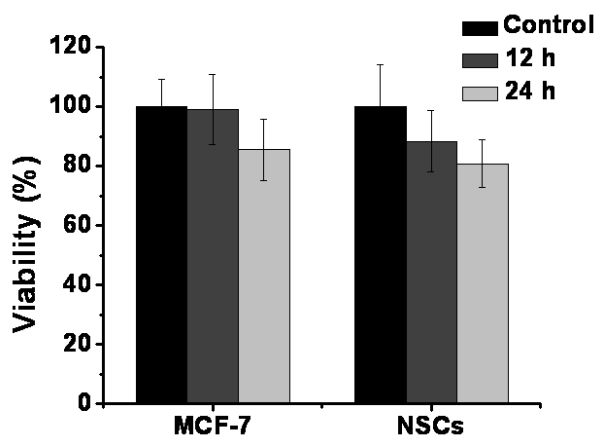


Fig. S22 Cytotoxicity of **LysoZn-1** on NSCs and MCF-7 cells. Cells were incubated with 1 μM **LysoZn-1** in FBS buffer for 12 h or 24 h, cell viabilities were examined using Thermo Fisher Scientific.

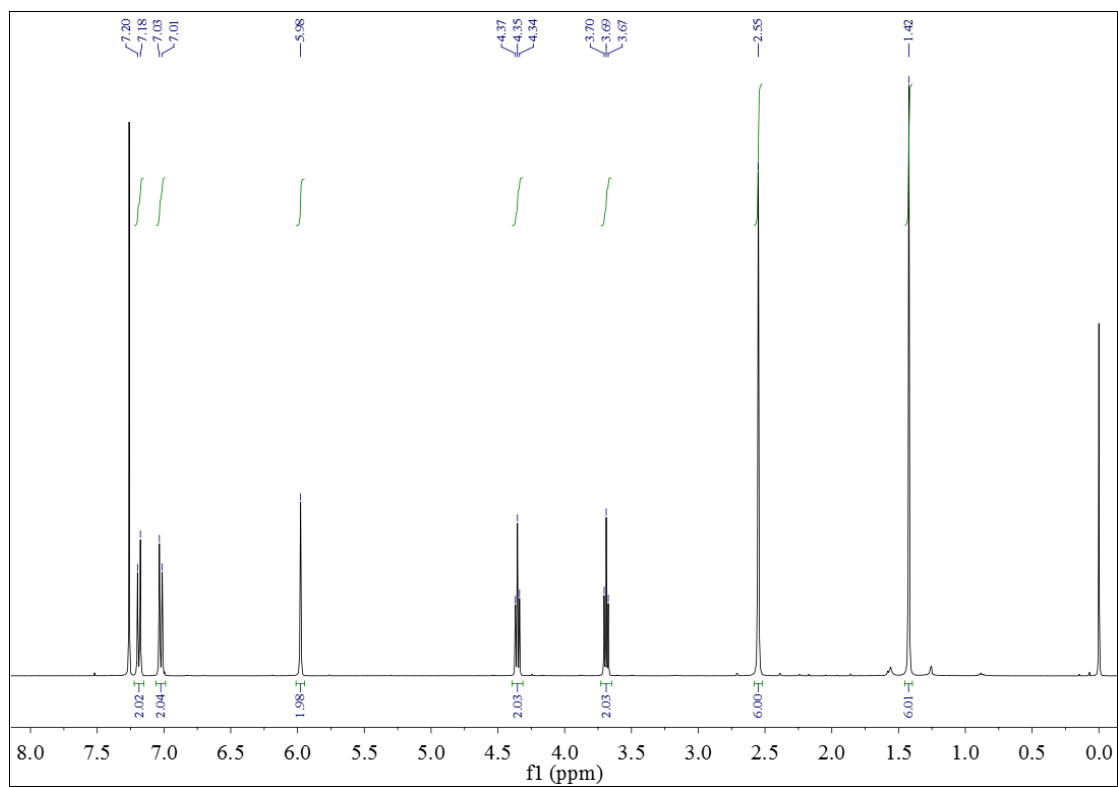


Fig. S23 $^1\text{H-NMR}$ of **2**

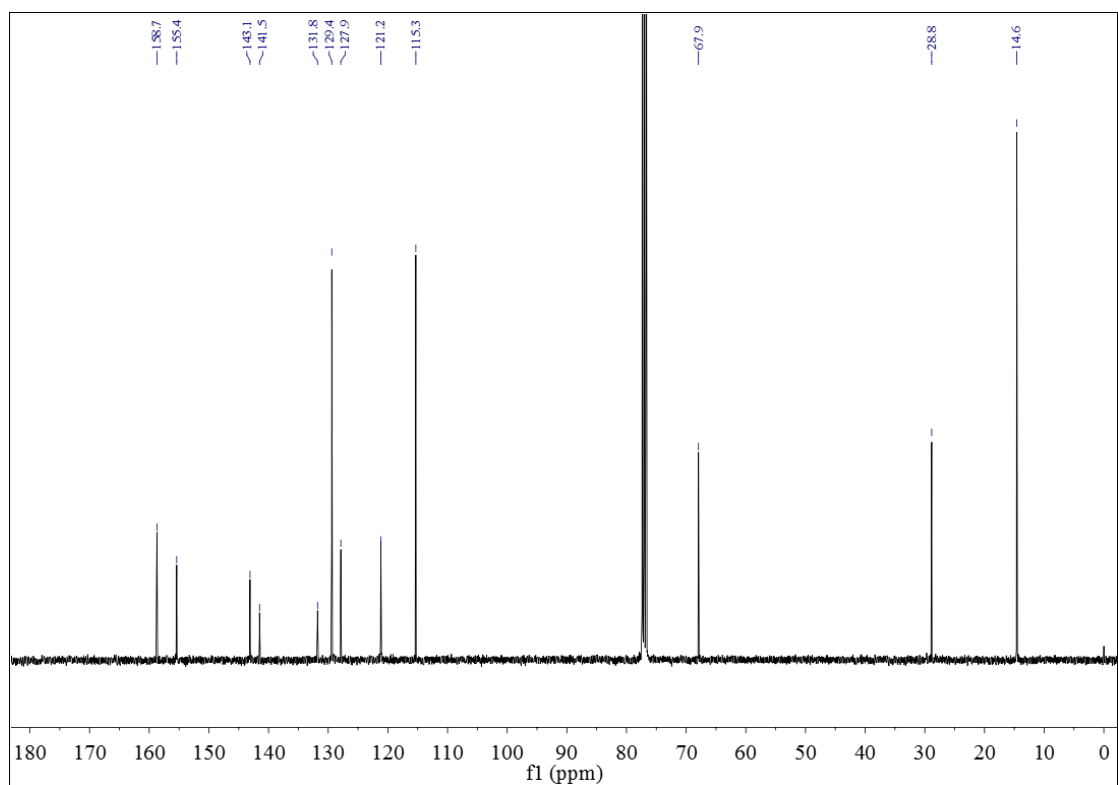


Fig. S24 $^{13}\text{C-NMR}$ of **2**

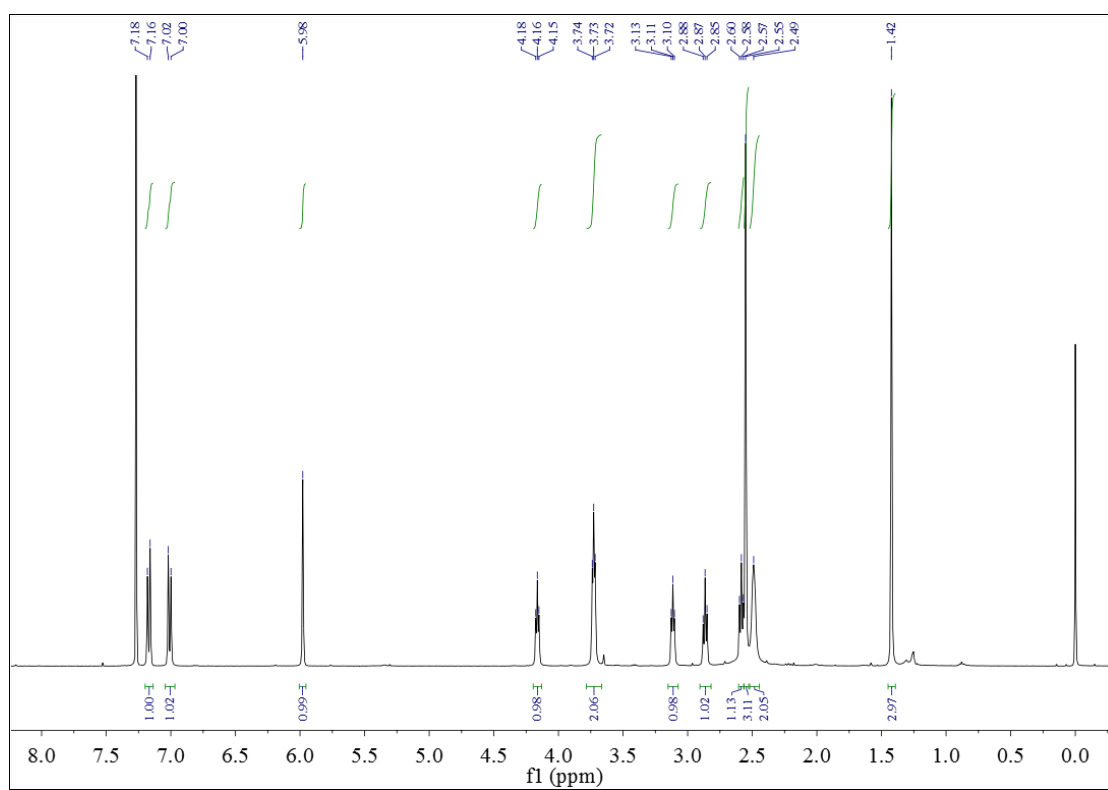


Fig. S25 $^1\text{H-NMR}$ of **3**

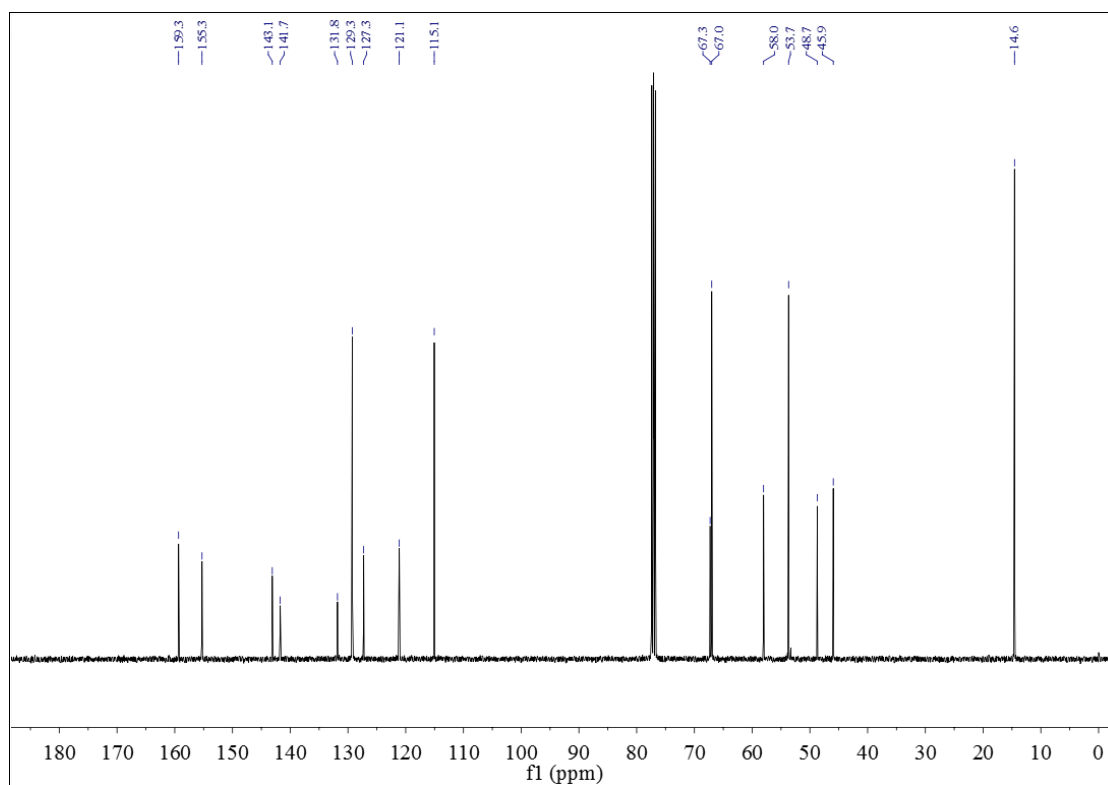


Fig. S26 $^{13}\text{C-NMR}$ of **3**

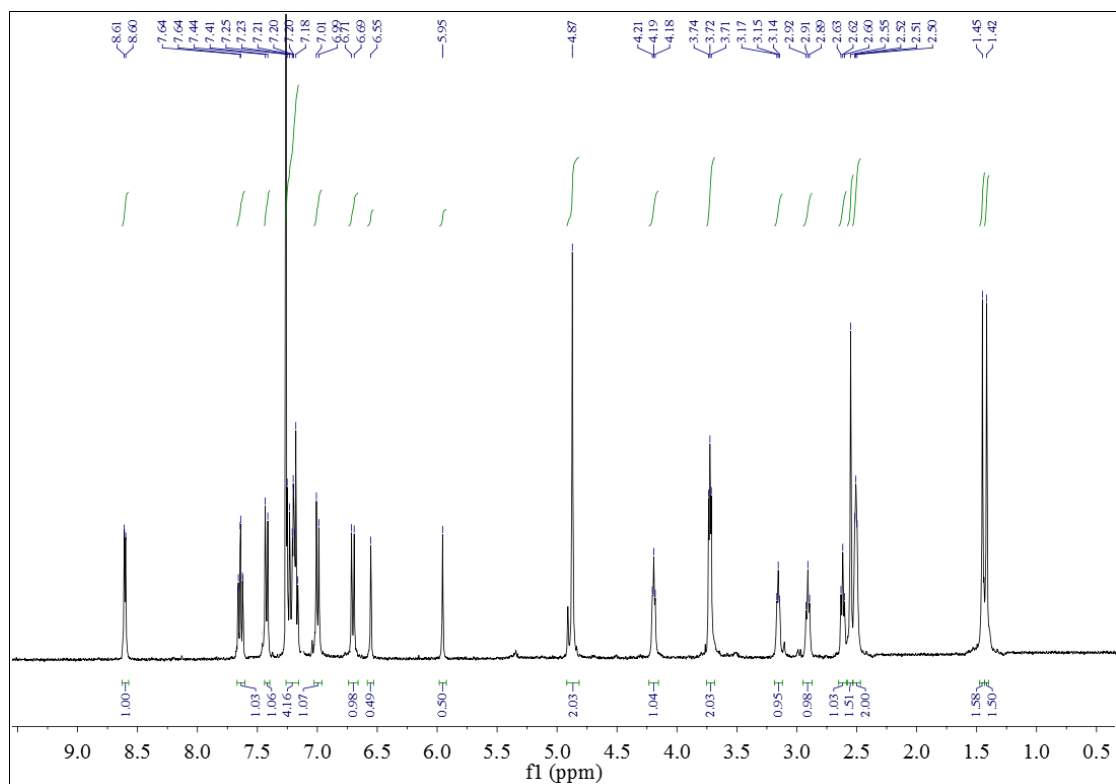


Fig. S27 ^1H -NMR of LysoZn-1

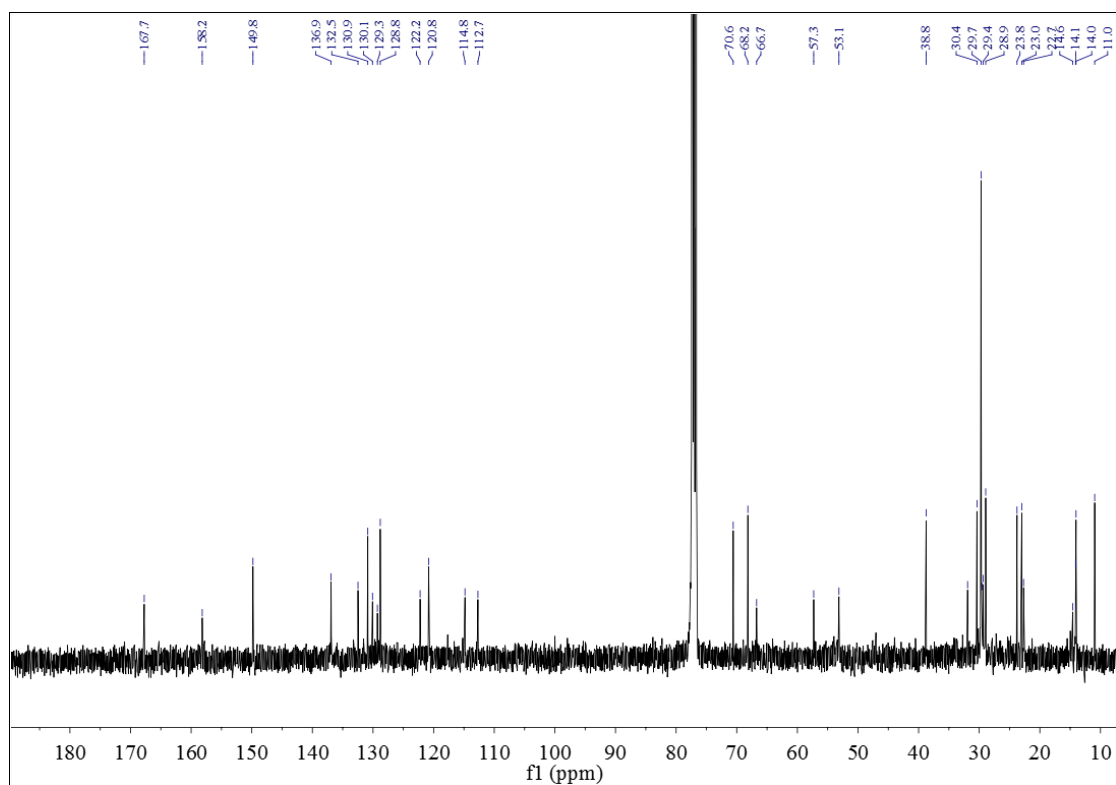


Fig. S28 ^{13}C -NMR of LysoZn-1

Reference